

Neopulmonary Outflow Tract Obstruction Assessment by 4D Flow MRI in Adults With Transposition of the Great Arteries After Arterial Switch Operation

Zahra Belhadjer, MD,^{1,2,3} Gilles Soulat, MD, PhD,^{1,3,4}  Magalie Ladouceur, MD, PhD,^{1,2,3,4}
Francesca Pitocco, MD,³ Antoine Legendre, MD,^{2,3} Damien Bonnet, MD, PhD,^{2,4}
Laurence Iserin, MD,^{2,3} and Elie Mousseaux, MD, PhD^{1,3,4*}

Background: The main complication in adult patients with transposition of the great arteries (TGA) treated by an arterial switch operation (ASO) is neopulmonary outflow tract stenosis (NPOTS). However, pulmonary flow velocity measurements cannot always be performed with transthoracic echocardiography (TTE) due to complex anatomical features. 4D flow MRI allows detection, quantification, and location of the obstruction site along the NPOTS.

Purpose and Hypothesis: To investigate the accuracy of 4D flow for the diagnosis of NPOTS in adults with TGA corrected by ASO.

Study Type: Prospective.

Population: Thirty-three adult patients with TGA treated by ASO (19 men, mean age 25.5 years old).

Field Strength/Sequence: Accelerated 4D flow research sequence at 3T.

Assessment: Maximum NPOTS velocities on TTE and 4D flow MRI done the same day.

Statistical Tests: Pearson correlation coefficient, paired *t*-test, and Bland–Altman analysis were used to investigate the relationship between TTE and MRI data.

Results: In 16 patients (48.5%), evaluation of NPOTS anatomy was not obtained by TTE, while it was always possible by 4D flow. Peak flow velocity (PV) measurements in Doppler and 4D flow were highly correlated ($r = 0.78$; $P < 0.001$). PV $> 350 \text{ cm}\cdot\text{s}^{-1}$ was detected in only one patient (3%) by TTE vs. five patients (15%) by 4D flow. Moreover, a high correlation was found between PV and the right ventricle (RV) mass index to body surface area when using 4D flow ($r = 0.63$; $P < 0.001$). The location of NPOTS was determined in all patients using 4D flow and concerned the main pulmonary artery in 42%.

Data Conclusion: Compared to TTE, 4D flow MRI provides better sensitivity to detect and locate NPOTS in patients with TGA treated by ASO. 4D flow PV measurements in NPOTS were well correlated with TTE PV and RV mass.

Level of Evidence: 1

Technical Efficacy: Stage 2

J. MAGN. RESON. IMAGING 2019.

TRANSPOSITION OF THE GREAT ARTERIES (TGA) is a rare congenital heart disease with an incidence of 1 per 1500 to 3000 live births, and accounts for 5–7% of congenital heart diseases.¹ Since the 1980s, patients with TGA most often undergo an arterial switch operation (ASO),

including transfer of the coronary arteries and translocation of the pulmonary artery by the Lecompte maneuver.² Long-term results after ASO are good, with an overall limited rate of complications which include proximal coronary artery stenosis, right ventricular outflow tract obstruction, and neo-aortic

View this article online at wileyonlinelibrary.com. DOI: 10.1002/jmri.27012

Received Jul 25, 2019, Accepted for publication Nov 19, 2019.

*Address reprint requests to: E.M., Paris-Cardiovascular Research Center; INSERM 970 56 rue Leblanc 75015 Paris, France. E-mail: elie.mousseaux@aphp.fr

From the ¹PARCC, INSERM 970, F-75015, Paris, France; ²Assistance Publique Hôpitaux de Paris, Hôpital Necker enfant malades, Centre de référence des Malformations Cardiaques Congénitales Complexes, M3C, F-75015, Paris, France; ³Université de Paris, F-75006, Paris, France; and ⁴Assistance Publique Hôpitaux de Paris, Hôpital Européen Georges Pompidou, F-75015, Paris, France

valve regurgitation.^{3,4} The more frequent complication in adult patients is neopulmonary outflow tract stenosis (NPOTS), leading to intervention in 15% of the ASO population.⁵⁻⁷ Intervention on NPOTS is recommended in symptomatic patients when systolic right ventricle (RV) pressure is over 60 mmHg (ie, peak velocity of tricuspid regurgitation [TR] >3.5 m/sec).⁸ However, systolic RV pressures are not always available in patients with undetected TR flow by transthoracic echocardiography Doppler (TTE), and the pulmonary flow measurement cannot always be obtained due to poor acoustic window and/or to the anteriorly positioned pulmonary artery.

Cardiac magnetic resonance imaging (MRI) is now recommended in the diagnosis and follow-up of adult patients with TGA after ASO,⁸ largely because of its ability to provide full coverage of both cardiac structures and great vessels.⁸⁻¹⁰ Nonetheless, it remains difficult to evaluate NPOTS by conventional 2D phase contrast imaging (2DPC) because it requires a good positioning of the slice, perpendicular to the flow at the location of peak velocity.¹¹

By using 3D velocity encoding phase contrast through time in a volume acquisition (4D flow MRI), these limitations could be overcome since a 3D dataset of velocity estimates is available, thus allowing a retrospective evaluation of blood flow with mean or peak velocity.¹²

The aim of the study was to investigate the accuracy and interobserver variability of 4D flow imaging to assess peak flow velocity (PV) along the NPOTS in adults after ASO. PVs of 4D flow MRI were compared to those obtained by transthoracic Doppler echocardiography, which is considered the noninvasive reference method to assess peak velocities. Furthermore, we also propose to compare the two

methods by analyzing the relationship between the severity of the NPOTS and RV hypertrophy.

Materials and Methods

Population

Thirty-three patients (19 male and 14 female) ages 18 to 35, who had ASO for TGA, followed at the adult congenital heart disease unit at European Hospital Georges Pompidou, were prospectively included between April 2015 and July 2016. Exclusion criteria consisted of the presence of any contraindication to perform an MRI.

The study was performed in accordance with the principles set out in the Declaration of Helsinki and was approved by the Ethics Review Board of our institution. All patients provided written informed consent to participate in the study

Transthoracic Echocardiography

Supravalvar and branch pulmonary artery stenosis were evaluated according ASE guidelines.⁹ Pulmonary Doppler interrogation of the severity at each level can be challenging with multiple levels of obstruction.

The position of the branch pulmonary arteries was seen in a high parasternal view. Assessment of the neopulmonary valve and supravalvar area was imaged from apical, parasternal, and subxiphoid windows. The best Doppler alignment was used for accurate estimates of pressure gradients through this area. Neopulmonary valve regurgitation was identified by color Doppler. All echocardiographic exams were performed and interpreted the same day as the MRI by two cardiologists (M.L. and L.L.) with respectively 15 and 25 years of experience in adults with CHD.

MRI

The acquisition protocol was designed to associate 4D flow imaging and a routine contrast MRI examination.

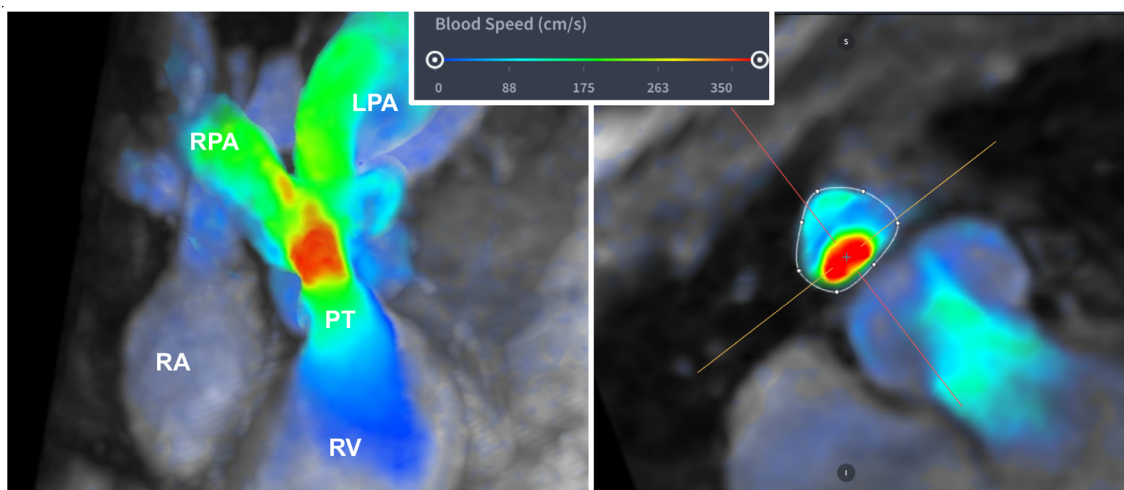


FIGURE 1: Peak velocity measurement in the pulmonary trunk using 4D flow MRI. Left panel: Illustration of a 3D velocity maximal intensity projection along the pulmonary ejection route at peak systole. Right panel: The manually-defined ROI is illustrated through the reformatted section perpendicular to the pulmonary trunk at peak systole obtained at the level of maximal velocity on 3D maximal intensity projection. Low velocities are color encoded in blue and high velocities in red.

MRI was performed by the same operator with 25 years of experience in MRI (E.M.), on a 70-cm wide-bore 3T system (GE Healthcare, Milwaukee, WI, Discovery 750w GEM) using a dedicated 32-channel phased-array cardiac surface coil and the same ECG-gated time-resolved 4D-flow MRI sequence. Steady-state free precession images were acquired in axial views, followed by long-axis and short-axis views of the left ventricle during successive breath-holds to cover the whole heart and great vessels, using the following scan parameters: acquisition matrix = 260×192 , field of view (FOV) = 320 to 360 mm, repetition time (TR) = 3.7 msec, echo time (TE) = 1.5 msec, flip angle = 50° , slice thickness = 8 mm, views per segment = 12. The short axis series was analyzed using QMass 8.0 (Medis, The Netherlands) by semiautomatic tracing of both endocardial and epicardial contours of the two ventricles. This was done by the same operator, blind to 4D flow results, to measure end-diastolic volume (EDV) and mass of each ventricle. A breath-hold 2D PC through-plane acquisition, orthogonal to the main pulmonary artery, was first acquired with a velocity encoding (Venc) equal to $350 \text{ cm}\cdot\text{sec}^{-1}$. Such acquisition was repeated with a higher Venc in case of aliasing.

A 0.2 mmol/kg of bodyweight injection of gadobenate dimeglumine (MultiHance, Bracco, Princeton, NJ) was given just before the 4D flow MRI acquisition and late gadolinium imaging was finally obtained between 12 and 15 minutes after injection.

4D Flow Acquisition and Postprocessing

An ECG-gated 4D flow sagittal orientation volume covering the entire mediastinum and the heart was acquired in all subjects. The Venc, similar in all three directions, was fixed to 350 or to $450 \text{ cm}\cdot\text{sec}^{-1}$. The choice of the Venc by the operator was based on the analysis of axial steady-state free precession (SSFP) images and initial results of the noncontrast-enhanced PC breath-hold acquisition used as a screening test. In the case of either small proximal pulmonary arteries or the presence of aliasing or high velocities, the Venc of the 4D flow MRI was fixed to $450 \text{ cm}\cdot\text{sec}^{-1}$. Scan parameters were as follows: average spatial resolution = $1.8 \times 1.5 \times 1.5 \text{ mm}$, flip angle 15° , TR = 4.2 msec, TE = 1.60 msec, bandwidth 62 kHz, views per segment = 2. The effective temporal resolution was 34 msec but the number of reconstructed heart phases after view-sharing was fixed to 50. Scan duration of 4D flow ranged from 8–12 minutes.

Postprocessing was performed using Arterys (San Francisco, CA). As illustrated in Fig. 1, using multiplanar reformatting, PV was localized along the pulmonary ejection route using the blood velocity maximal intensity projection of a thin volume. Then a region of interest (ROI) was manually drawn on the section perpendicular to the vessel of interest at the location of highest velocities in the main, the right, and the left pulmonary artery.

PV measurements were done independently by two observers with 1 and 5 years of experience in cardiac imaging, blind to ventricular volume estimates.

Statistical Analysis

Baseline characteristics are provided as mean \pm SD or median (interquartile range) when appropriate for continuous variables, and percentages \pm SD for discrete variables. Normality was checked using the Shapiro–Wilk test. Univariate correlations between 4D flow and Doppler pulmonary velocity measurements as well as interobserver variability were reported using Pearson correlation coefficients and

TABLE 1. Population Characteristics

Characteristics	N = 33
Age (y)	25.5 \pm 4.9
Gender Male	19 (58%)
Weight (kg)	66 \pm 13
Height (cm)	171 \pm 11
BSA (cm^2)	1.73 \pm 0.19
BMI ($\text{kg}\cdot\text{cm}^{-2}$)	22.6 \pm 3.56
Heart rate (bpm)	71 \pm 11
Brachial systolic blood pressure (mmHg)	124 \pm 11
Brachial diastolic blood pressure (mmHg)	72 \pm 6
TTE Parameters	
Full RVOTO assessment	17 (52%)
RVOTO Peak velocity ($\text{cm}\cdot\text{s}^{-1}$)	240 [185–325]
RVOTO Peak velocity > $350 \text{ cm}\cdot\text{s}^{-1}$	1/33 (3%)
End systolic interventricular septum flattening	8 (24%)
MRI parameters	
LV EDVi ($\text{ml}\cdot\text{m}^{-2}$)	76 \pm 18
LV ESVi ($\text{ml}\cdot\text{m}^{-2}$)	30 \pm 9
LVEF (%)	61 \pm 6
LV MASSi ($\text{g}\cdot\text{m}^{-2}$)	56 \pm 12
RV EDVi ($\text{ml}\cdot\text{m}^{-2}$)	86 \pm 25
RV ESVi ($\text{ml}\cdot\text{m}^{-2}$)	37 \pm 15
RVEF (%)	58 \pm 8
RV MASSi ($\text{g}\cdot\text{m}^{-2}$)	18 [16–21.5]
Pulmonary route estimation	33 (100%)
RVOTO Peak velocity ($\text{cm}\cdot\text{s}^{-1}$)	187 [164–260]
RVOTO Peak velocity > $350 \text{ cm}\cdot\text{s}^{-1}$	5/33 (15%)

Results are presented as mean \pm SD, number (%), or median [interquartile range].

BSA: body surface area; BMI: body mass index; HR: heart rate; LV left ventricle; EDVi: end diastolic volume indexed to BSA; ESVi: end systolic volume indexed to BSA; EF: left ventricular ejection fraction; MASSi: mass indexed to BSA.

the intraclass correlation coefficient; differences were estimated using a paired *t*-test, as they were normally distributed, and displayed with a Bland–Altman plot. According to the guidelines for intervention,

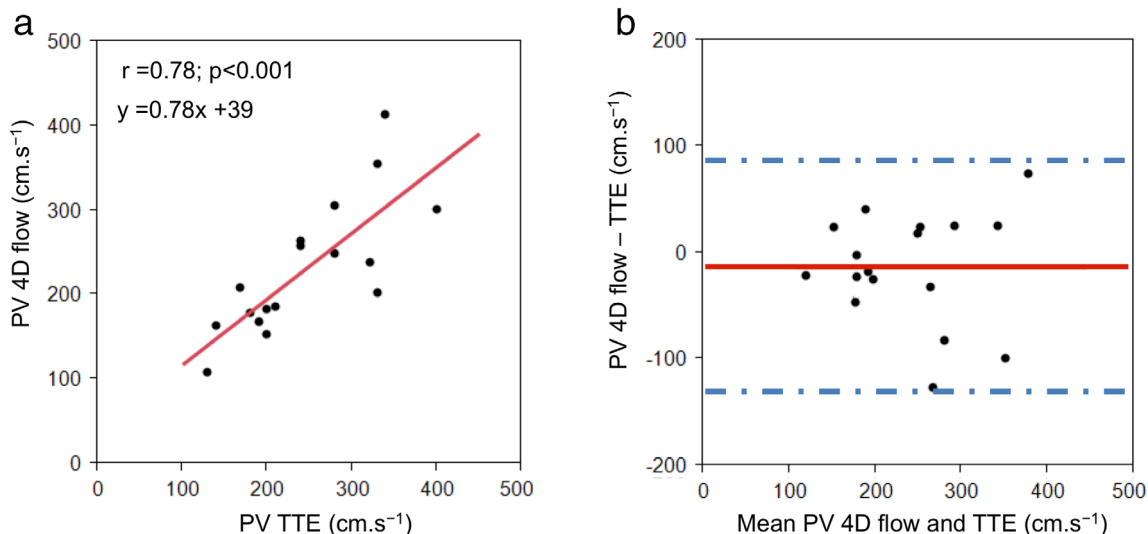


FIGURE 2: Correlation of NPOTS Peak velocity (PV) assessed by 4D flow MRI and TTE. Scatterplot (a) and Bland–Altman plot (b) show agreement between the two methods.

the cutoff of 350 m.s⁻¹ was used for the two imaging methods to detect severe NPOTS. Relationships between PV with NPOTS and right ventricular mass were assessed using the Pearson correlation coefficient for the two imaging techniques.

$P < 0.05$ was used to indicate statistical significance. Analyses were done using JMP 10 (SAS Institute, Cary, NC).

Results

Baseline characteristics of the 33 patients are summarized in Table 1.

PV measurements all along the NPOTS were possible in all patients using 4D flow MRI; meanwhile, these measurements were only obtained in 17 patients (52%) using TTE. PV obtained with 4D flow MRI and TTE were well correlated ($r = 0.79$, $P < 0.001$, Fig. 2a). Mean PV was 245 ± 78 cm.s⁻¹ in TTE, and 224 ± 82 cm.s⁻¹ in 4D flow MRI. However, the difference was not significant (-14.6 cm.s⁻¹ ± 12.7 , $P = 0.26$) and without any bias as illustrated in the Bland–Altman plot, while 95% limits of agreements were $[-121 -90$ cm.s⁻¹] (Fig. 2b). The intraclass correlation coefficient between TTE and MRI was 0.77. Due to poor acoustic window or image quality, in 16 patients (48.5%), flow velocity measurements were not available all along the NPOTS including pulmonary arteries when using TTE and Doppler, whereas they were obtained in all ASO patients using 4D flow MRI. TTE succeeded in detecting significant NPOTS, meaning a PV >350 cm.s⁻¹, in 1/33 patient (3%), and 4D flow detected a PV >350 cm.s⁻¹ in 5/33 patients (15%). The four patients with only 4D flow detection had an end systolic interventricular septum flattening in TTE; three patients with end systolic interventricular septum flattening had PV <350 cm.s⁻¹ both in TTE and 4D flow.

An example of a patient with Left Pulmonary Artery stenosis is illustrated in Fig. 3, showing the main issue

encountered for TTE to have the ultrasound beam well aligned with the direction of maximal velocities in case of TGA corrected by ASO after a Lecompte maneuver.

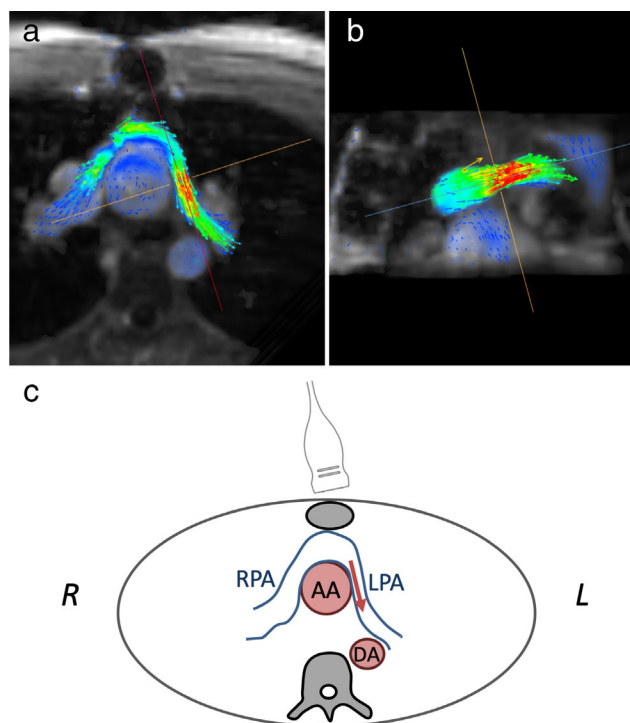


FIGURE 3: Illustration of the difficulties encountered by TTE operators in aligning the ultrasound beam with the direction of maximum velocities in proximal pulmonary arteries. Axial (a) and coronal (b) 4D flow MRI shows acceleration of the flow through proximal arteries with high velocities (in red); the corresponding arrow indicates the direction of such velocities. As shown in (a) with the superimposition of the red line illustrating the direction of the proximal left pulmonary artery branch, as well as in diagram (c), the ultrasound beam must cross the sternum to be properly aligned with the direction of the main flow. In this particular patient, maximal velocity was underestimated by 70 cm.s⁻¹ in TTE compared to MRI (R: Right; L: Left).

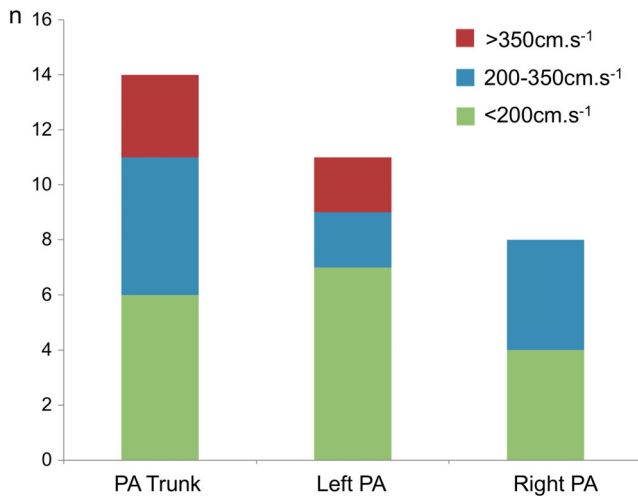


FIGURE 4: Distribution of the peak velocity locations along the NPOTS and their corresponding values obtained by using 4D flow MRI in all 33 subjects. PA = pulmonary artery; n = number of subjects per location.

Distribution of PV locations along the NPOTS is shown in Fig. 4. PVs were found in the main pulmonary artery in 42%, in left pulmonary artery branch in 34%, and in right pulmonary artery branch in 24%.

Relationship With RV Hypertrophy

PVs were significantly correlated with RV hypertrophy as estimated by RV mass indexed to body surface area (BSA) for both TTE ($r = 0.56$; $P = 0.02$) and 4D flow MRI ($r = 0.63$; $P < 0.001$) (Fig. 5a,b). PVs estimated by 4D flow MRI were still strongly correlated with RV mass index when only the 17 patients with a contributive TTE ($r = 0.71$; $P < 0,001$) were taken into account.

Interobserver Variability

A good agreement between PV measurements of the two observers was obtained ($r = 0.97$, $P < 0.001$) with a mean difference of $-0.41 \pm 3.40 \text{ cm.s}^{-1}$ ($P = \text{NS}$) as shown in Fig. 6. The interobserver variability coefficient for PV was 4.4% and intraclass correlation coefficient was 0.97.

Discussion

By using 4D flow MRI to assess peak velocity, we could better detect and precisely locate NPOTS velocities in adult patients with ASO than by using standard echocardiography Doppler. 4D flow MRI allowed detection of a higher proportion of patients with a significant obstruction ($PV >350 \text{ cm.s}^{-1}$) compared to TTE. When PVs were available by using Doppler, we found a good correlation between the two cardiac imaging modalities for estimating peak velocity along the NPOTS.

The better sensitivity of MR may be related to the ability of 4D flow MRI to provide a complete volume assessment of the heart and great vessels. By evaluating the three spatial components of the velocity vector, the 4D flow MRI is more likely to give the maximum velocity compared with Doppler, which requires the ultrasonic beam to be well aligned in the jet direction during ventricular ejection. Beyond an image quality that is not always satisfactory in the analysis of the RV ejection pathway in many adult subjects, aligning this ultrasound beam in the direction of the main flow is a major problem. Indeed, the direction of the jet changes during the cardiac cycle and may be incompatible with the available acoustic window.

Finally, we found a significant relationship between 4D flow MRI PVs and RV mass. This result confirms the close

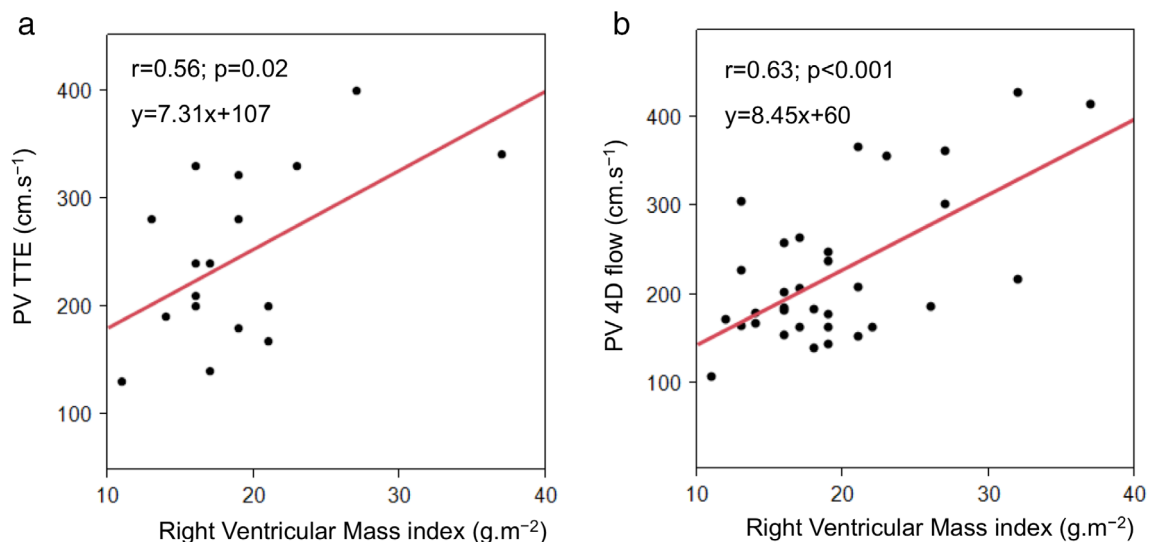


FIGURE 5: Linear correlation between NPOTS PV and right ventricle mass indexed to BSA. Estimation of PV by TTE ($N = 17$) in (a), and by 4D flow MRI in (b) ($N = 33$).

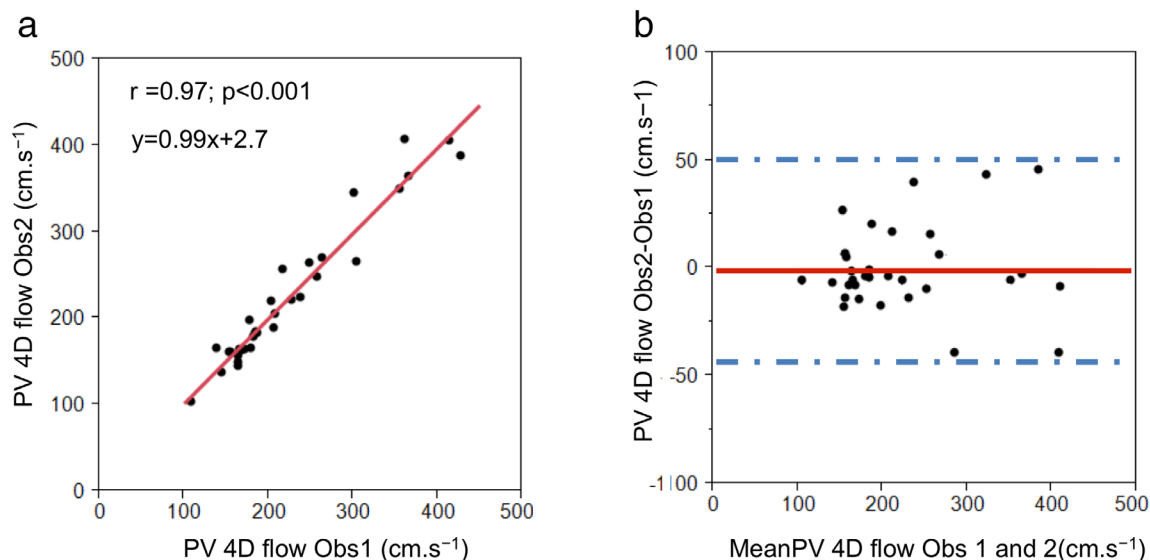


FIGURE 6: Comparison of interobserver 4D flow MRI NPOTS PV measurement. Scatterplot (a) and Bland–Altman plot (b) show agreement between the two observers.

physiological relationship between RV hypertrophy and the afterload level of the RV. However, by getting a significant relationship between RV mass and 4D flow MRI PVs, we confirmed the accuracy of 4D flow MRI to detect NPOTS. Additionally, all patients with a PV >350 $\text{cm}\cdot\text{s}^{-1}$ in 4D, but a noncontributing Doppler also had a flattening of the interventricular septum in TTE during systole, which indicates the relevance of the high-velocity values measured by the 4D flow.

To our knowledge, only one study previously investigated the ability of 4D flow to assess NPOTS maximal velocity after ASO¹³ in a pediatric TGA population.¹³ In 19 young subjects (mean age 13 years) with nonconcomitant TTE, the authors found a good agreement between echocardiography and 4D flow MRI PVs assessed by using maximal velocity detected by using maximal intensity projection of velocities estimated within volume including NPOTS and pulmonary arteries. In the adult congenital heart disease population, we confirm that the detection of significant stenosis of the NPOTS using TTE remains challenging.^{13,14} Indeed, a complete evaluation of the NPOTS by TTE could be obtained in only 52% of our adult patients. In contrast, by using 4D flow MRI, we showed that 4D flow MRI could assess PVs along the NPOTS in all patients and we detected a significant obstruction in 15% of cases. Finally, by using the maximal velocity projection within a thin volume covering the entire length of the NPOTS and the manual determination of an ROI orthogonal to the flow at the visual location, we found a good interobserver reproducibility in PV measurements. Our results confirm previous reports that highlighted that 4D flow could be useful for clinical purposes in other congenital heart diseases and that the additional scan time required is counterbalanced by avoiding multiples 2D PC acquisition at different locations along the NPOTS.^{15–17}

With phase contrast methods, peak velocity estimates are less sensitive to eddy current effects than flow volume estimates. However, the choice of the Venc is essential. In the present study, the choice of the Venc was based on the size of the proximal pulmonary arteries or the presence of aliasing or high velocities detected by breath-hold fast 2D PC acquisitions. In the future, multi-Venc acquisition could help to avoid aliasing by combining a low Venc acquisition with a high velocity-to-noise ratio and a high Venc to obtain an accurate aliasing correction.

Study Limitations

Invasive pressure measurements were not available in our cohort and could not be compared to 4D flow measurements. We did not design the study to indicate intervention on the NPOTS, and we did not correlate our 4D flow MRI estimate with functional parameters. We used only PVs to evaluate the increased RV afterload and its relationship with RV hypertrophy. PVs only reflect the transvalvular pressure drop at peak systole, when the temporal pressure can be neglected. However, as previously suggested,¹⁸ better RV afterload indices could be used if the transpulmonary valve pressure drop is estimated during the entire systole by using the general Navier–Stokes equation that includes the convective acceleration and viscous effects of the flow. Such new approaches have been recently proposed by estimating either noninvasive pressure difference mapping¹⁹ or absolute pixelwise absolute pressures derived from 4D flow MRI data in the aortic arch.²⁰ Helical flow pattern analysis within pulmonary arteries²¹ or other complex indices derived from turbulent kinetic energy^{22,23} could also be very useful in the future to access the right ventriculo-arterial coupling.²⁴ Even if reproducibility between observers was good here, it would be desirable to reduce the dependence of operators in the analysis by

proposing an automated segmentation of the NPOTS and detection of the maximum velocity along this tract.¹³

In conclusion, after using a 10-minute 4D flow MRI volume acquisition in free breathing, we found good agreement between MRI and TTE PVs measurements obtained in adult TGA patients after ASO. PVs in 4D flow MRI were also well related to RV hypertrophy. Thanks to its full anatomical coverage, 4D flow MRI could quantify a higher proportion of NPOTS than TTE and help determine the accurate anatomy of the NPOTS in all ASO patients. Further studies are required to determine the prognostic value and the impact of 4D flow MRI in the management of TGA patients after ASO.

Acknowledgment

Z.B. received a grant from the Fondation medical de recherche and the Association pour la recherche en cardiologie du Foetus à l'adulte for an MSc Fellowship

References

- Brickner ME, Hillis LD, Lange RA. Congenital heart disease in adults. Second of two parts. *N Engl J Med* 2000;342:334–342.
- Lecompte Y, Zannini L, Hazan E, et al. Anatomic correction of transposition of the great arteries. *J Thorac Cardiovasc Surg* 1981;82:629–631.
- Angeli E, Raisky O, Bonnet D, Sidi D, Vouhé PR. Late reoperations after neonatal arterial switch operation for transposition of the great arteries. *Eur J Cardiothorac Surg* 2008;34:32–36.
- Khairy P, Clair M, Fernandes SM, et al. Cardiovascular outcomes after the arterial switch operation for D-transposition of the great arteries. *Circulation* 2013;127:331–339.
- Williams WG, Quaegebeur JM, Kirklin JW, Blackstone EH. Surgery for congenital heart disease. *Cardiovasc Surg* 1997Dec;114(6):975–987.
- Hutter PA, Krebs DL, Mantel SF, Hitchcock JF, Meijboom EJ, Bennink GBWE. Twenty-five years' experience with the arterial switch operation. *J Thorac Cardiovasc Surg* 2002;124:790–797.
- Shepard CW, Germanakis I, White MT, Powell AJ, Co-Vu J, Geva T. Cardiovascular magnetic resonance findings late after the arterial switch operation. *Circ Cardiovasc Imaging* 2016;9:e004618.
- Endorsed by the Association for European Paediatric Cardiology (AEPC), Authors/Task Force Members, Baumgartner H, et al. ESC guidelines for the management of grown-up congenital heart disease (new version 2010): The Task Force on the Management of Grown-up Congenital Heart Disease of the European Society of Cardiology (ESC). *Eur Heart J* 2010;31:2915–2957.
- Cohen MS, Eidem BW, Cetta F, et al. Multimodality imaging guidelines of patients with transposition of the great arteries: A report from the American Society of Echocardiography developed in collaboration with the Society for Cardiovascular Magnetic Resonance and the Society of Cardiovascular Computed Tomography. *J Am Soc Echocardiogr* 2016;29:571–621.
- Kilner PJ, Geva T, Kaemmerer H, Trindade PT, Schwitler J, Webb GD. Recommendations for cardiovascular magnetic resonance in adults with congenital heart disease from the respective working groups of the European Society of Cardiology. *Eur Heart J* 2010;31:794.
- Nayak KS, Nielsen J-F, Bernstein MA, et al. Cardiovascular magnetic resonance phase contrast imaging. *J Cardiovasc Magn Reson* 2015;17.
- Dyverfeldt P, Bissell M, Barker AJ, et al. 4D flow cardiovascular magnetic resonance consensus statement. *J Cardiovasc Magn Reson* 2015;17.
- Jarvis K, Vonder M, Barker AJ, et al. Hemodynamic evaluation in patients with transposition of the great arteries after the arterial switch operation: 4D flow and 2D phase contrast cardiovascular magnetic resonance compared with Doppler echocardiography. *J Cardiovasc Magn Reson* 2016;18.
- Morgan CT, Mertens L, Grotenhuis H, Yoo S-J, Seed M, Grosse-Wortmann L. Understanding the mechanism for branch pulmonary artery stenosis after the arterial switch operation for transposition of the great arteries. *Eur Heart J Cardiovasc Imaging* 2017;18:180–185.
- Hsiao A, Lustig M, Alley MT, Murphy MJ, Vasanaawala SS. Evaluation of valvular insufficiency and shunts with parallel-imaging compressed-sensing 4D phase-contrast MR imaging with stereoscopic 3D velocity-fusion volume-rendered visualization. *Radiology* 2012;265:87–95.
- Valverde I, Nordmeyer S, Uribe S, et al. Systemic-to-pulmonary collateral flow in patients with palliated univentricular heart physiology: Measurement using cardiovascular magnetic resonance 4D velocity acquisition. *J Cardiovasc Magn Reson* 2012;14:10–1186.
- Vasanaawala SS, Hanneman K, Alley MT, Hsiao A. Congenital heart disease assessment with 4D flow MRI: CHD assessment for 4D flow. *J Magn Reson Imaging* 2015;42:870–876.
- Falahatpisheh A, Rickers C, Gabbert D, et al. Simplified Bernoulli's method significantly underestimates pulmonary transvalvular pressure drop: General vs. simplified Bernoulli equation. *J Magn Reson Imaging* 2016;43:1313–1319.
- Rengier F, Delles M, Eichhorn J, et al. Noninvasive 4D pressure difference mapping derived from 4D flow MRI in patients with repaired aortic coarctation: Comparison with young healthy volunteers. *Int J Cardiovasc Imaging* 2015;31:823–830.
- Bargiotas I, Redheuil A, Evin M, et al. Pixel-wise absolute pressures in the aortic arch from 3D MRI velocity data and carotid artery applanation tonometry. *IEEE* 2014;5105–5108.
- Reiter G, Reiter U, Kovacs G, Olschewski H, Fuchsjäger M. Blood flow vortices along the main pulmonary artery measured with MR imaging for diagnosis of pulmonary hypertension. *Radiology* 2015;275:71–79.
- Francois CJ, Srinivasan S, Schiebler ML, et al. 4D cardiovascular magnetic resonance velocity mapping of alterations of right heart flow patterns and main pulmonary artery hemodynamics in tetralogy of Fallot. *J Cardiovasc Magn Reson* 2012;14:16.
- Geiger J, Hirtler D, Bürk J, et al. Postoperative pulmonary and aortic 3D haemodynamics in patients after repair of transposition of the great arteries. *Eur Radiol* 2014;24:200–208.
- Aubert R, Venner C, Huttin O, et al. Three-dimensional echocardiography for the assessment of right ventriculo-arterial coupling. *J Am Soc Echocardiogr* 2018;31:905–915.